Article

# Ni nano buffer layer provides light-weight CNT/Cu fibers with superior robustness, conductivity and ampacity

Jingyun Zou, Dandan Liu, Jingna Zhao, Ligan Hou, Tong Liu, Xiaohua Zhang, Yonghao Zhao, Yuntian Zhu, and Qingwen Li

*ACS Appl. Mater. Interfaces*, **Just Accepted Manuscript** • DOI: 10.1021/acsami.7b19012 • Publication Date (Web): 12 Feb 2018

# Ni nano buffer layer provides light-weight CNT/Cu fibers with superior robustness, conductivity and ampacity

*Jingyun Zou,*[†,‡] *Dandan Liu,*[‡] *Jingna Zhao,*[‡] *Ligan Hou,*[‡] *Tong Liu,*[¶] *Xiaohua Zhang,*[‡]* *Yonghao Zhao,*[†] *Yuntian T. Zhu*[†,§]* *and Qingwen Li*[‡]*

[†] Nano Structural Materials Center, School of Materials Science and Engineering, Nanjing University of Science and Technology, Nanjing 210094, China

[‡] Division of Advanced Nano-Materials, Suzhou Institute of Nano-Tech and Nano-Bionics, Chinese Academy of Sciences, Suzhou 215123, China

[¶] Vacuum Interconnected Nanotech Workstation, Suzhou Institute of Nano-Tech and Nano-Bionics, Chinese Academy of Sciences, Suzhou 215123, China

[§] Department of Materials Science & Engineering, North Carolina State University, Raleigh, NC 27695, USA

KEYWORDS: carbon nanotube, composite fiber, buffer layer, interfacial bonding, electroplating, ampacity

ABSTRACT: Carbon nanotube (CNT) fiber has not shown its advantage as next-generation light-weight conductor due to the large contact resistance between CNTs, as reflected by its low conductivity and ampacity. Coating CNT fiber with a metal layer like Cu has become an effective solution to this problem. However, the weak CNT-Cu interfacial bonding significantly limits the mechanical and electrical performances. Here we report that a strong CNT-Cu

interface can be formed by introducing a Ni nano buffer layer before depositing the Cu layer. The Ni nano buffer layer remarkably promotes the load and heat transfer efficiencies between the CNT fiber and Cu layer, and improves the quality of the deposited Cu layer. As a result, the new composite fiber with a 2-μm-thick Cu layer can exhibit a super-high effective strength >800 MPa, electrical conductivity $>2 \times 10^7$ S/m, and ampacity $>1 \times 10^5$ A/cm$^2$. The composite fiber can also sustain 10000 times of bending and continuously work for 100 h at 90% ampacity.

## INTRODUCTION

Carbon nanotube (CNT) is one of the most promising candidates for next-generation conductors owing to its extremely high strength,[1] electrical conductivity,[2,3] ampacity,[4,5] thermal conductivity,[6] low density,[7] and good corrosion resistance.[8] However, due to the weak van der Waals interaction[9,10] and remarkable electron and phonon scattering between CNTs,[11,12] there is a significant sacrifice of mechanical, electrical and thermal properties when CNTs are assembled into macroscopic structures, such as one-dimensional (1D) fiber,[13,14] 2D film,[15] and 3D bulk.[16] For CNT fiber, the electrical conductivity is usually $10^4$–$10^5$ S/m,[17] and various chemical modifications have been carried out to improve the conductivity, such as acid oxidation,[18,19] iodine doping,[20,21] auric/platinic acid treatment,[22] and ozone irradiation.[23] However, the improvement is still limited and the highest conductivity was $6.74 \times 10^6$ S/m, about one order of magnitude smaller than that of pure copper.[20] Furthermore, the Joule heating effect suppresses strongly the ampacity of CNT assemblies.[5] The measured value of $1.4 \times 10^4$ A/cm$^2$ for a CNT fiber[0] is far below the ultimate value $\approx 10^9$ A/cm$^2$ for a single CNT.[4,5] Nevertheless, the CNT fiber's tensile strength can exceed 2–3 GPa,[25,26] much stronger than metal wires. Therefore, improving the electrical properties is of great importance, with great challenges as well.

As a solution, it is feasible to simultaneously utilize the advanced performances of CNT and metal by making them into a composite material. For example, by electrodepositing a Cu layer on CNT films, a CNT-Cu composite conductor was obtained with a high conductivity of $4.7 \times 10^7$ S/m.[27] It also showed an extremely high ampacity of $6 \times 10^8$ A/cm$^2$, two orders of magnitude higher than that of conventional metals.[27] In another study, a continuous fabrication of highly conducting CNT/Cu fiber was realized by combining CNT fiber spinning and Cu electrodeposition.[19] Another similar treatment of physical vapor deposition was also used to realize the high-performance CNT-Cu composite fibers.[28] However, the poor wettability between carbon and copper leads to the weak interfacial bonding between the deposited Cu layer and CNT fiber.[29] Furthermore, the weak conjugation between Cu *d*-orbitals and C π-electrons causes a high interfacial contact resistance.[29,30] Thus, both the mechanical and electrical performance of CNT/Cu composite fibers are strongly limited.

An intermediate that has good affinity with both CNT and Cu can be a solution to such problem. In this paper, by introducing Ni nano buffer layer, the tensile strength, electrical conductivity, ampacity, and long-term stability of CNT/Cu composite fiber can be remarkably improved.

## RESULTS AND DISCUSSIONS

**Interface design.** The CNT/Cu composite fiber was prepared based on the continuous electrodeposition of several-μm-thick Cu layer around a CNT fiber.[19] Three different Cu-CNT interfaces were introduced to the pristine, anodic oxidized, and Ni-coated CNT fibers, namely the CNT-Cu, CNT-O-Cu, and CNT-Ni-Cu interfaces, respectively (see schematic Figure 1a). The oxidization was realized by the electrochemical anodization,[19] and the Ni buffer layer was coated on a pristine fiber by a quick online electrodeposition (Figure S1). The level of oxidation

and the amount of Ni atoms were controlled by adjusting the voltage of the anodization and Ni plating. The optimized voltages were 5 V and 3 V for the Ni plating and anodization treatment (detailed discussed in Figure S2 and Figure S3), respectively. Here the Ni mass fraction was just ≈0.5 wt% according to the mass increase after the treatment. After then, for all the three fibers, a Cu plating process was performed continuously. After the deposition, an annealing treatment at 300 °C was performed to eliminate the Cu crystal defects for better performance.

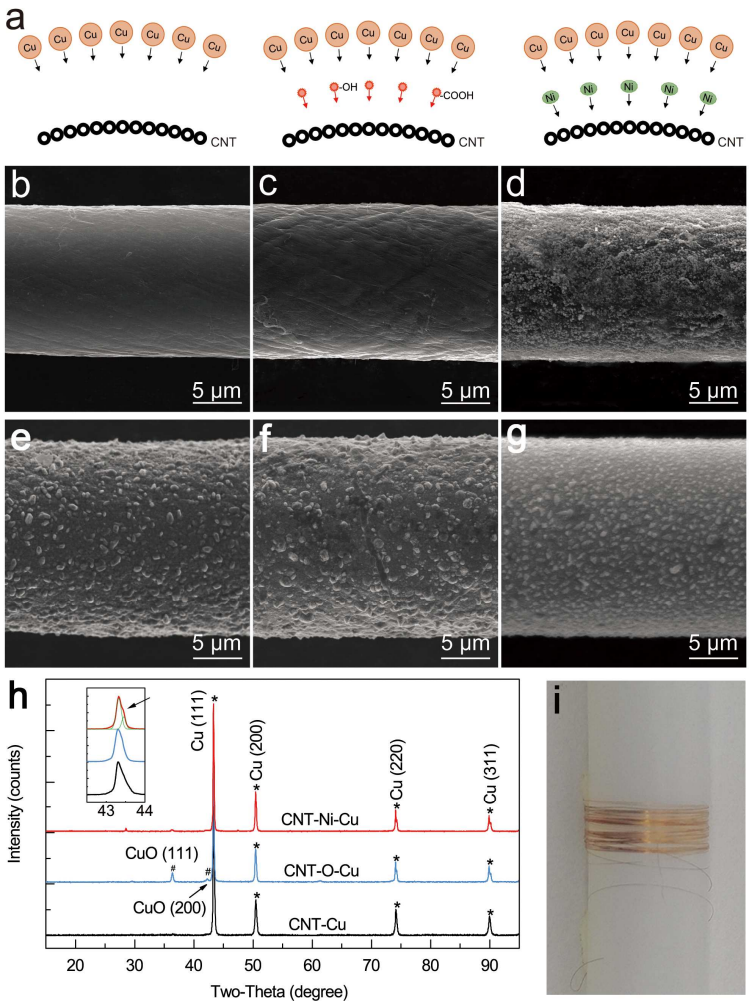


**Figure 1.** Preparation and characterization of CNT/Cu composite fibers. (a) Schematic of three depositions. (b-d) SEM images of surface morphology of the original, anodized and Ni-treated CNT fiber. (e-f) The surface morphologies after the Cu deposition, of the CNT-Cu, CNT-O-Cu and CNT-Ni-Cu fiber, respectively. (h) XRD patterns of the CNT-Cu, CNT-O-Cu and CNT-Ni-

Cu samples. (i) A CNT/Cu fiber with Ni buffer layer, collected on an 8-mm-diameter winder and annealed, still showed metallic lustre after being placed in air for more than one month.

Figure 1b-g compares the surface morphology of CNT fiber before and after the Cu deposition. The anodization and Ni treatment converted the fiber surface from smooth to rough (Figure 1b-d), corresponding to the formation of oxygen-containing functional groups[19] and Ni nanoparticles. These modified fiber surface could affect the following Cu deposition; it strongly affected the Cu crystalline structure, see Figure 1e-g, indicating that the crystallinity, grain size, and packing density of Cu particles can differ greatly.

First, X-ray diffraction (XRD) revealed that cubic copper was deposited on the pristine fiber surface, as reflected by the sharp (111), (200), (220), and (311) peaks (Figure 1h). On the surface containing functional groups, small but clear peaks of CuO (111) and (200) lattices were observed, corresponding to a covalent anchoring of Cu seeds around these groups. Quite differently, Ni nanoparticles changed the Cu crystallinity by forming a certain alloy interfaces. By magnifying the Cu (111) peak, one can find a strong shoulder peak at 43.5°, 0.2° above the pristine peak (inset Figure 1h). This revealed that Ni atoms had diffused into Cu particles, and caused a slight compression of the Cu crystals, mostly between the (111) lattices.[31]

Second, by using the Debye-Scherrer equation on the XRD results, the Cu grain sizes were calculated as 29.0, 59.4 and 57.5 nm in the CNT-Cu, CNT-O-Cu and CNT-Ni-Cu fibers, respectively (Table S1). On the pristine fiber surface, there were no preferential active sites to anchor Cu seeds, and thus it was difficult to grow large-sized Cu particles. Therefore, an assembly with rich grain boundaries was formed (as also reflected by the smallest conductivity as discussed below). On the contrary, Cu atoms can nucleate around the active functional groups and the Ni seeds, to induce a faster growth toward large-sized Cu particles, see schematic Figure S4.

Thus, as a result, the deposited Cu layers were also different in mass density. For example, after coating a 2-μm-thick Cu layer on a 15-μm-diameter fiber (mass density ≈1.01 g/cm$^3$), the final mass density was 3.40, 3.61 and 3.83 g/cm$^3$ for the CNT-Cu, CNT-O-Cu and CNT-Ni-Cu fibers, corresponding to a Cu fraction of 81.6, 82.8 and 83.7 wt%, respectively. By dividing the mass increase by the increase in cross-sectional area, from the diameter change, the density of Cu layer was 7.36, 7.94 and 8.50 g/cm$^3$ for the three samples, respectively. Interestingly, owing to the high density (very close to the ideal copper density of 8.96 g/cm$^3$), the CNT-Ni-Cu sample even showed metallic lustre after being placed in air for more than one month (Figure 1i), corresponding to an improved oxidation resistance.

**Mechanical performance.** A micro-droplet test[32] was used to evaluate the interfacial bonding strength (IFBS) between the Cu layer and core CNT fiber (Figure 2a). A series of epoxy resin beads were coated, and the uncovered Cu layer was etched by a dilute sulphuric acid. The strong adhesion between epoxy and Cu ensured the sliding to take place just between CNT and Cu. IFBS is calculated by dividing the detach force by the contact area.

With increasing the embedded length, IFBS generally decreased (Figure 2b), as the possibility increased to meet weak interfacial contacts that can cause shell-to-fiber sliding by avalanche effect. Thus, for a better comparison, a same embedded length of 500 μm was used to evaluate the effect of surface treatment. The CNT-Cu sample exhibited an average IFBS ≈ 2.9 MPa and ≈ 2.0 MPa before and after the 300-°C annealing, indicating that the interface was not thermally stable. For the CNT-O-Cu, although the initial IFBS was even higher (≈3.5 MPa), the interface became much worse by heating, as its IFBS dropped greatly down to ≈1.9 MPa. Fortunately, the Ni buffer layer exhibited superior interfacial robustness, as it not only enhanced the IFBS up to 3.59 MPa, but also well maintained the IFBS (3.61 MPa) after the annealing.

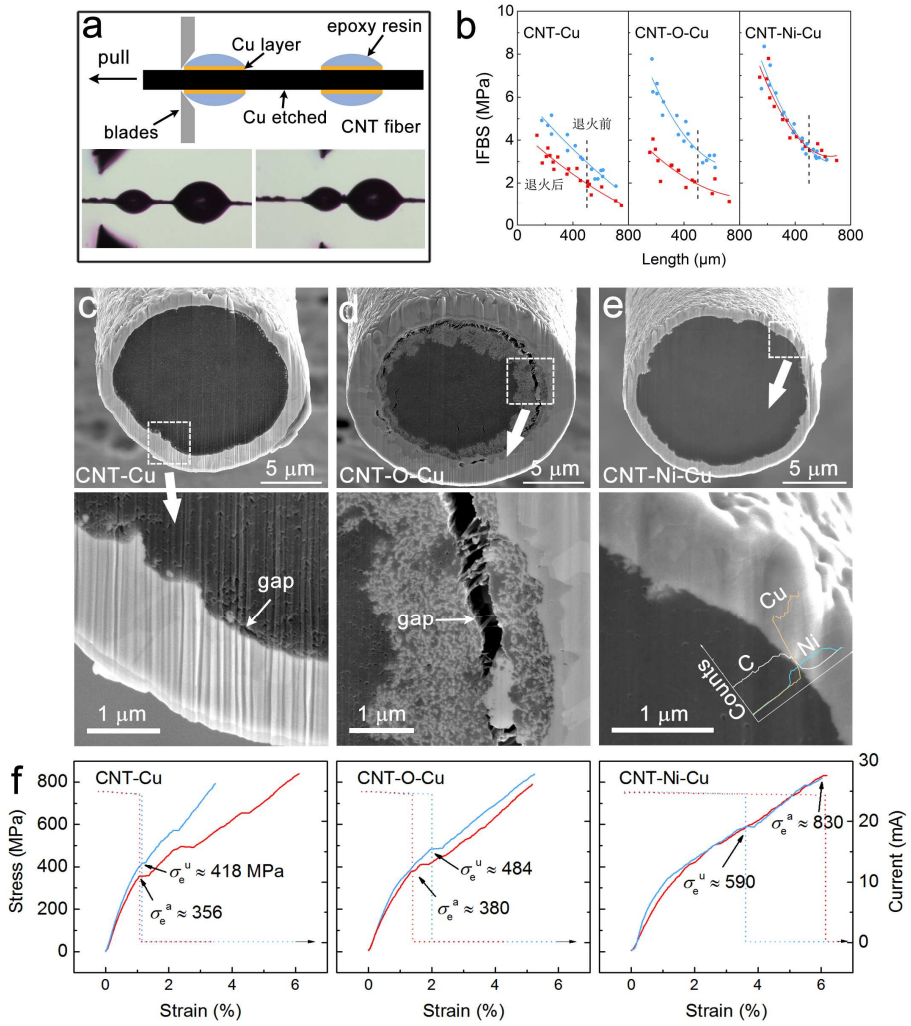


**Figure 2.** Effect of surface treatment on the mechanical properties of CNT/Cu composite fibers. (a) Schematic of a micro-droplet test and the sample preparation. Two snapshots are provided to show the slippage of one epoxy bead. (b) IFBS as a function of embedded length for the CNT-Cu, CNT-O-Cu and CNT-Ni-Cu fibers before (blue) and after (red) the annealing. The dashed lines correspond to the results at embedded length of 500 μm. (c-e) SEM images of the cross sections and interfaces for the annealed fibers. The inset in (e) shows the interfacial C/Cu/Ni element distribution in the CNT-Ni-Cu fiber, obtained with an EDS line scanning. (f) Stress-strain and current-strain curves for different fibers before and after the annealing. The sample length was 6 mm and a voltage of 0.01 V was applied. The effective strengths ($\sigma_e^u$ and $\sigma_e^a$ are for the unannealed and annealed samples) are labelled by arrows.

Figure 2c-e showed the cross sections of the three annealed fibers, cut by focused ion beam (FIB). There existed clear gaps at the CNT-Cu and CNT-O-Cu interfaces, acting as the main reason for the reduced IFBS. On the contrary, no gaps or voids were observed with the presence of Ni buffer layer. More importantly, the energy-dispersive x-ray spectroscopy (EDS) line

scanning showed that Ni had diffused into both the Cu layer and CNT fiber, nearly up to a depth of 1 μm. (The effect of annealing on the Ni diffusion is shown in Figure S5.) The penetration could cause compression on Cu lattices, in very good agreement with the XRD characterization (Figure 1h). Furthermore, the diffusion can act as a "generalized" surface sizing,[32] to bind the Cu layer and the core fiber tightly, effectively avoiding the localized stress concentration. As a result, its tensile property can be remarkably improved and maintained.

For the composite fiber, the tensile properties can be described by the ultimate tensile strength ($\sigma_f$) that both CNT core and Cu layer have fractured, and also by an effective tensile strength ($\sigma_e$) where only the Cu layer fractures.[19] Up to $\sigma_e$, the tensile stress could still further increase, while the electric current, by applying a constant voltage, would drop to nearly zero due to the lack of conducting paths.

Owing to the high strength of the core CNT fiber, the three samples all exhibited $\sigma_f \approx 800$ MPa (Figure 2f). However, $\sigma_e$ was only 418 and 484 MPa for the unannealed CNT-Cu and CNT-O-Cu fibers. It became even worse, dropping to 356 and 380 MPa, after the annealing, in agreement with the reduction in IFBS. The situation changed totally for the Ni treatment. Before the annealing, $\sigma_e$ was already up to 590 MPa, corresponding to the strongest IFBS. Surprisingly, the annealing could even increase $\sigma_e$ up to 830 MPa, as high as nearly the ultimate strength, much higher than a similar CNT-Cu fiber (515 MPa) obtained through the physical vapor deposition.[28] This could be another strong evidence for the efficiency of the diffused Ni buffer layer after the annealing. As the strength of nanocrystalline copper is usually below 500 MPa,[33] such high $\sigma_e$ is obviously an effect of the enhanced IFBS.

The fracture morphologies of these samples well demonstrated the variation of IFBS and $\sigma_e$ (Figure S6). For the CNT-Cu and CNT-O-Cu fibers, the fracture was usually a sword-sheath

pull-out where many CNT bundles were peeled off due to the interfacial contacts. But after the annealing, few CNT bundles were peeled off due to the reduced IFBS. Differently, the pull-out length was significantly shortened owing to existence of Ni buffer layer before the annealing, and the outer Cu layer and the core CNT fiber finally broke nearly simultaneously for the annealed CNT-Ni-Cu fiber.

The CNT-Ni-Cu fiber was also highly bendable owing to the high IFBS. After being bended for 10000 cycles (8 s per cycle), with an amplitude of 0.5 cm for 1 cm fiber length (see inset Figure 3a), its electrical resistance did not grow up but even decreased during the first ≈3000 cycles (Figure 3a). Such fiber was also highly flexible, as a knot did not affect the resistance, as there was no cracks in Cu layer (Figure 3b). For the CNT-O-Cu fiber with un-improved interface, the resistance started to increase after ≈4000 cycles, showing a limited bendability. The situation was even worse for a pure Cu wire, as its resistance continuously increased during flexure testing, and the wire fractured after only ≈2200 cycles due to bending-induced workhardening.

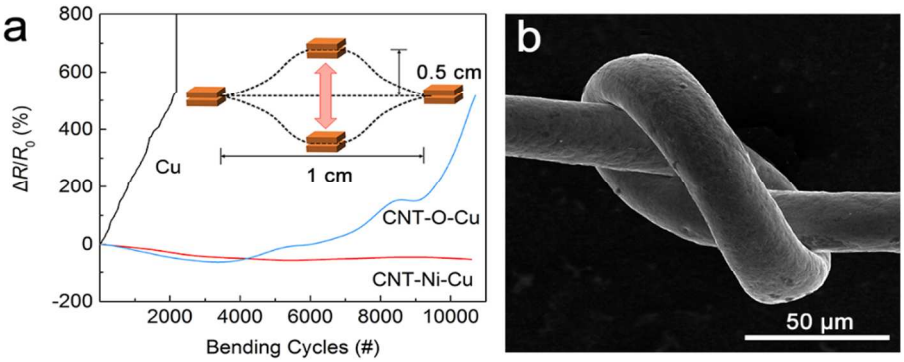


**Figure 3.** Stability and flexibility of CNT/Cu composite fibers. (a) Percentage change in resistance of the CNT-Ni-Cu, CNT-O-Cu and pure Cu fibers observed as a function of bending cycles. Inset: schematic of the bending test apparatus. (b) SEM image of a tightly knotted CNT-Ni-Cu fiber.

**Electrical performance.** The conductivity strongly depends on the deposited structure of Cu layers. The larger grain size, the higher conductivity. It was $(0.67 \pm 0.03) \times 10^7$ and $(0.93 \pm$

0.04) × $10^7$ S/m for the unannealed CNT-Cu and CNT-O-Cu fibers, respectively (Figure 4a). For the unannealed CNT-Ni-Cu fiber, it further increased up to (1.45 ± 0.06) × $10^7$ S/m, possibly owing to the compact Cu layer as reflected by the higher mass density of 8.50 g/cm$^3$.

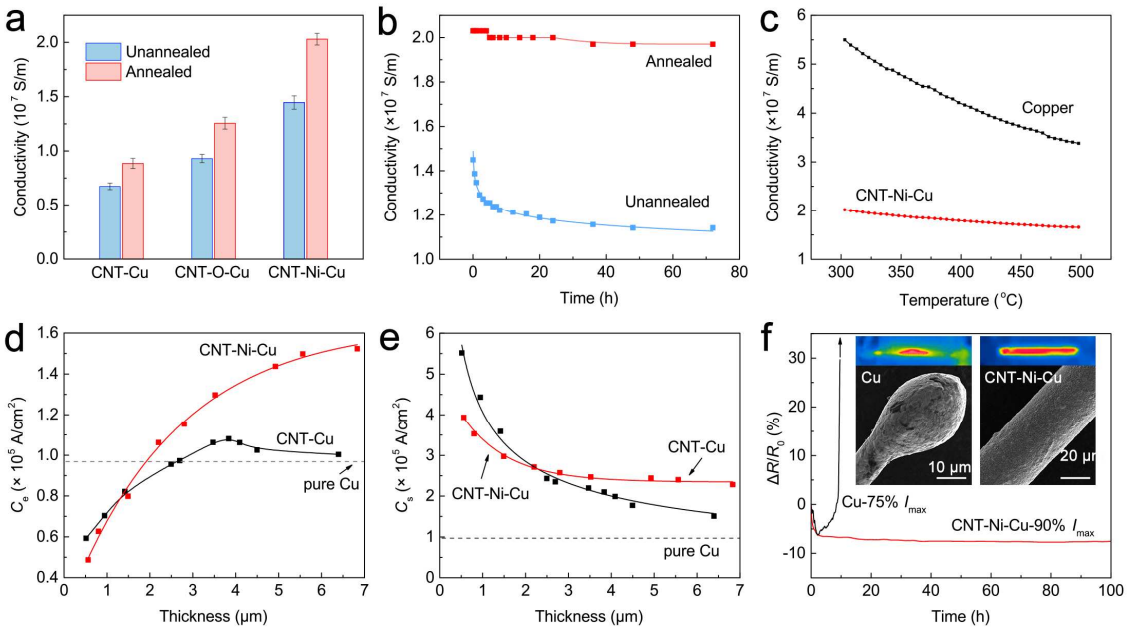


**Figure 4.** Electrical properties of CNT/Cu composite fibers. (a) Conductivity of the CNT-Cu, CNT-O-Cu and CNT-Ni-Cu fibers before and after the annealing. (b) Evolution of conductivity with time for two CNT-Ni-Cu fibers in air. (c) A comparison of temperature-dependent conductivity between a CNT-Ni-Cu fiber and a Cu wire. (d,e) Ampacity ($C_e$ and $C_s$, see the main text) as a function of Cu thickness for the annealed CNT-Cu and CNT-Ni-Cu fibers. (f) Resistance change versus time for a Cu wire and an annealed CNT-Ni-Cu fiber upon carrying a high current. The insets are the thermal imaging figures, together with images of the fused Cu wire and the undamaged CNT-Ni-Cu fiber.

After the annealing, the grains grew much bigger (see Table S1) and thus the conductivity all increased correspondingly, up to (0.89 ± 0.05) × $10^7$, (1.26 ± 0.06) × $10^7$, and (2.03 ± 0.05) × $10^7$ S/m for the three composite fibers (Figure 4a). These values were all obtained at a Cu thickness of 2 μm. For the best conductivity, the value was already 36% IACS at an overall mass density of 3.7 g/cm$^3$ (41% of bulk Cu).

The annealing also improved the oxidation resistance. The conductivity of an unannealed CNT-Ni-Cu sample droped greatly upon being placed in air, by ≈14% in just 4 h and ≈22% after

72 h (Figure 5b). After the annealing, the grain size increased and grain defects could be eliminated, the fiber became much stable againt oxidation. After 72 h, the conductivity decreased just by 3%, from $2.03 \times 10^7$ to $1.97 \times 10^7$ S/m.

Furthermore, as compared to Cu wire, the CNT-Ni-Cu fiber had also a low temperature coefficient of resistivity (TCR). As increasing temperature from 300 K to 500 K, the conductivity of Cu wire decreased from $5.5 \times 10^7$ to $3.05 \times 10^7$ S/m, corresponding to a TCR of $4.12 \times 10^{-3}$ $K^{-1}$, while the TCR was only $1.14 \times 10^{-3}$ $K^{-1}$ for the composite fiber, as its decrease in conductivity was just from $2.03 \times 10^7$ to $1.66 \times 10^7$ S/m (Figure 5c). Possibly, as discussed recently, the CNTs not only participate the conduction, but also change the electron scattering from complete inelastic to partial elastic at the contact with $sp^2$ lattices.[34]

The current carrying capacity, ampacity, is another important electrical property for CNT/Cu composites.[27] It can be described by the entire fiber's ampacity $C_e$ or the Cu shell's ampacity $C_s$, by dividing the maximum current a fiber can carry by the cross-sectional area of the fiber or of the Cu shell, respectively. (Typical *I-V* curves are shown in Figure S7.) At a Cu thickness of 2 μm, $C_e = 0.91 \times 10^5$ A/cm$^2$ for the annealed CNT-Cu fiber, and was lower than that of the pure Cu wire ($0.97 \times 10^5$ A/cm$^2$, commercial ultra-fine copper wire, 20 μm in diameter, 99.9% purity). It became much higher ($1.06 \times 10^5$ A/cm$^2$) after the introduction of Ni buffer layer and annealing (Figure 4d). By further considering the overall mass density, the corresponding specific ampacity of the CNT-Ni-Cu fiber could be up to $4.24 \times 10^4$ and $3.45 \times 10^4$ A·cm/g at a Cu thickness of 2 and 5 μm, respectively, while it was only $1.09 \times 10^4$ A·cm/g for the Cu wire.

As the Cu layer carries the most part of the current, one can also compare the ampacity of the Cu layer, $C_s$, between the composite fibers and the Cu wire (Figure 4e). $C_s$ of the two

composite fiber both exceeded greatly that of the Cu wire, and when the Cu layer thickness exceeded 2 μm, the CNT-Ni-Cu exhibited better performances as reflected by the nearly constant $C_s$. This reveals the advantage of intimate contact between the CNT fiber and Cu layer. For example, the high thermal conductivity of the core fiber allows the quick transfer and disspation of the Joule heat generated in the Cu layer, and thus avoids the localized overheating. Such effect can be well demonstrated by the morphologies of the fused fibers (see Figure S8). For the CNT-Cu and CNT-O-Cu fibers, by increasing the current slightly up to the ampacity, the Joule heating-induced high temperature damaged the interface (see Figure 2c and 2d), and finally caused the Cu layer to fuse, leaving the core fiber intact. On the contrary, as the interface was much thermally stable for the CNT-Ni-Cu fiber, the Cu layer could postpone its fusing until the core CNT fiber burnt.

The CNT-Ni-Cu fiber was very stable when carrying large currents as compared to Cu wires. When a current of 255 mA (≈90% ampacity) was applied, the former's resistance was well maintained without any increase for more than 100 h in air, while the Cu wire's resistance grew up rapidly at a current of 208 mA (≈75% ampacity) and gradually fused in less than 10 h (Figure 4f). This is owing to the high thermal conductivity of the CNT fiber, because it can rapidly conduct the Joule heat along the whole fiber to avoid localized heat concentration. From the inset Figure 4, one can find the temperture distribution was quite homogeneous along the CNT-Ni-Cu fiber, while there was a localized high temperature segment in the Cu wire. (Notice that, as the samples were not optimally annealed and exposed to air for hours, the resistances both decreased slightly due to the electrothermal induced annealing within the initial 2 h.)

**Demo application.** The high conductivity of the composite fiber can be used in various ways. For example, several LED lights can be connected in series and got lit under a small

current of several mA (Figure 5a). Multi-ply composite fibers can be used as a conducting rope to lift and light a heavy and high-power bulb (Figure 5b). Interestingly, the composite fiber can be developed as a lighting device. By exposing a small segment of the core CNT fiber, the electric current will get concentrated at this segment to induce a lightening effect. Thus, the composite fiber can act as a device integrating the conductor and incandescent filament together (Figure 5c). And it has worked for over 24 h without any damage.

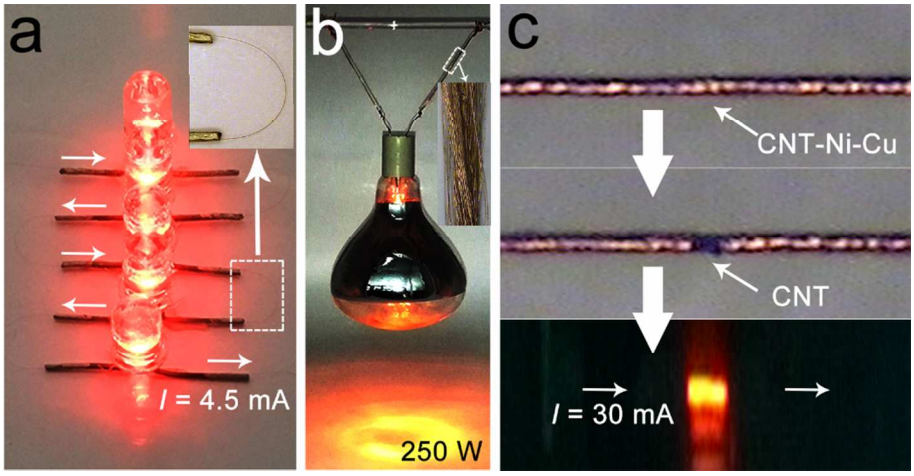


**Figure 5.** Demo applications of CNT/Cu composite fibers. (a) Four LED lights in series, connected by CNT-Ni-Cu fibers, are activated under a current of 4.5 mA. (b) A 250-W bulb lit and suspended by 100-ply CNT-Ni-Cu fibers. (c) By peeling off a small segment of Cu layer from the CNT-Ni-Cu composite fiber, such segment can be lit under conducting a current of 30 mA, acting as an integrated lighting.

## CONCLUSIONS

In this paper, we demostrate a high-performance CNT/Cu composite fiber by introducing a Ni nano buffer layer. The Ni layer facilitates the Cu deposition process, producing larger Cu grains, compact Cu layer and strong interfacial bonding. Both mechanical and electrical properties can be improved owing to the good cooperation of the CNT fiber and Cu layer in transferring load, heat and current. This produces a CNT-Ni-Cu fiber with an effective strength of 830 MPa and a high conductivity of $2.03 \times 10^7$ S/m at a mass density of 2.51 g/cm$^3$. Such composite fiber exhibits superior performances in terms of bendability, TCR, ampacity and long-term stability.

EXPERIMENTAL SECTION

**Preparation of CNT fiber.** The CNT fiber was prepared by the forest-based spinning.[7,35] The forest with a height of about 250 μm were grown on the silicon substrate through chemical vapor deposition,[0] and most of the CNTs were 2–4-walled (diameter ≈ 4–7 nm) as shown in Figure S9a. A 1.5-μm wide sheet was drawn from the forest and processed into a uniform and strong CNT fiber through online twisting and solvent shrinking,[36,37] with a diameter of 15 μm, a twisting angle of 20°, a strength of 1.21 ± 0.05 GPa and a modulus of 40.2 ± 3.2 GPa (Figure S9b,c). Its electrical conductivity is 430-520 S/cm, close to the result reported previously.[19,22]

**Preparation of CNT/Cu composite fibers.** The CNT-Ni-Cu composite fiber was prepared through continuous electrodeposition method (Figure S1). The deposition time of the Ni and Cu plating was same as they were performed in two bathes with the same structure. The Ni buffer layer was plated in the solution containing 120 g/L $NiCl_2$ and 200 ml/L HCl using a 5-V constant voltage. The Cu layer was deposited using a 5-V impulse voltage (generating a current of ≈1.2 mA) in the solution contained 160 g/L $CuSO_4 \cdot 5H_2O$, 12 ml/L $H_2SO_4$ (98%), and 1 ml/L octylphenyl poly-(ethylene glycol) ether (n = 10) (OP-10). The deposited thickness of the Cu layer were controlled by the rolling speed as shown in Figure S10. To deposit a 2-μm-thick Cu layer, the collecting speed was about 25 rpm, corresponding to a Ni/Cu deposition time of 25 s.

To prepare the CNT-O-Cu fiber, a anodization treatment was carried out in a 10% $H_2SO_4$ solution with a 3-V constant voltage (generating a current of ≈0.03 mA) to replace the Ni plating. And the CNT-Cu fiber was frabricated by depositing Cu on the pristine CNT fiber (the Ni plating or anodization treatment were removed). After then, the annealing treatment was carried out in Ar (gas flow 300 sccm) at the optimal temperature of 300 °C for 30 minutes (Figure S11).

**Characterization.** The IFBS was measured by a modified micro-droplet test, with an HM410 Equipment for Evaluation of Fiber/Resin Composite Interface Properties (Tohei Sangyo Co., Ltd., Tokyo, Japan). The tensile tests were performed by using a T150 Universal Testing Machine (Keysight Technologies, Inc., Santa Rosa, USA), equipped with a 500-mN load cell. All of the samples were mounted on paper templates with a gauge length of 6 mm, and the tensile rate was 0.001 $s^{-1}$. The bending performance were evaluated on an Instron 3365 Universal Test Machine (Instron Corp., Norwood, USA), with an up-down moving speed of 2.5 mm/s. The electrical conductivity and ampacity were measured by a Keithley 4200A-SCS parameter analyzer (Tektronix Inc., Beaverton, USA) and a Zive BP2 power system (WonATech Co. Ltd., Seoul, Korea), respectively. A Fluke TiS60 thermal imaging camera (Fluke Corporation, American Fork, USA) was used for processing thermal images of the CNT-Ni-Cu and pure CU wires when large currents were carried.

A Quanta 400 FEG SEM (FEI, Hillsboro, USA), a D8 Advance XRD (Bruker AXS, Karlsruhe, Germany), a Scios DualBeam FIB system (FEI, Hillsboro, USA) and an Octane Super EDS (EDAX Inc., Mahwah, USA) were used to characterize and analyze the composite structures. The fiber diameter was measured by optical diffraction using a 532 nm laser,[0] and the Cu thickness was calculated by the increase in diameter; they both were further confirmed by SEM. The mass density was measured by an XP2U high-precision analytical balance (Mettler-Toledo LLC., Columbus, USA).

## ASSOCIATED CONTENT

**Supporting Information**.

Continuous online electrodeposition; detailed XRD information; schematics of the copper deposition process; analysis of the CNT-Ni-Cu interface; morphologies of the fractured and fused fibers; current density-voltage curves; details of the CNT fiber; optimizing of the Ni deposition parameter; control of Cu thickness and fiber density; effect of the annealing treatment (PDF)

## AUTHOR INFORMATION

### Corresponding Author

*(X.Z.) Email: xhzhang2009@sinano.ac.cn

*(Y.T.Z.) Email: ytzhu@ncsu.edu

*(Q.L.) Email: qwli2007@sinano.ac.cn

### Notes

The authors declare no competing financial interest.

## ACKNOWLEDGMENT

We thank financial supports from the National Natural Science Foundation of China (21503267, 21473238, 51561145008), Youth Innovation Promotion Association of the Chinese Academy of Sciences (2015256), and National Key Research and Development Program of China (2016YFA0203301). We also thank the Vacuum Interconnected Nanotech Workstation Vacuum of Suzhou Institute of Nano-Tech and Nano-Bionics for the FIB characterization.

## REFERENCES

(1) Yu, M.-F.; Lourie, O.; Dyer, M. J.; Moloni, K.; Kelly, T. F.; Ruoff, R. S., Strength and Breaking Mechanism of Multiwalled Carbon Nanotubes Under Tensile Load. *Science* **2000,** *287* (5453), 637-640.

(2) Ebbesen, T.; Lezec, H.; Hiura, H.; Bennett, J.; Ghaemi, H.; Thio, T., Electrical conductivity of individual carbon nanotubes. *Nature* **1996,** *382*, 54-56.

(3) Li, H. J.; Lu, W.; Li, J.; Bai, X.; Gu, C., Multichannel ballistic transport in multiwall carbon nanotubes. *Phys. Rev. Lett.* **2005,** *95* (8), 086601.

(4) Yao, Z.; Kane, C. L.; Dekker, C., High-Field Electrical Transport in Single-Wall Carbon Nanotubes. *Phys. Rev. Lett.* **2000,** *84* (13), 2941-2944.

(5) Wei, B. Q.; Vajtai, R.; Ajayan, P. M., Reliability and current carrying capacity of carbon nanotubes. *Appl. Phys. Lett.* **2001,** *79* (8), 1172-1174.

(6) Berber, S.; Kwon, Y.-K.; Tománek, D., Unusually High Thermal Conductivity of Carbon Nanotubes. *Phys. Rev. Lett.* **2000,** *84* (20), 4613-4616.

(7) Zhang, X. F.; Li, Q. W.; Holesinger, T. G.; Arendt, P. N.; Huang, J. Y.; Kirven, P. D.; Clapp, T. G.; DePaula, R. F.; Liao, X. Z.; Zhao, Y. H.; Zheng, L. X.; Peterson, D. E.; Zhu, Y. T., Ultrastrong, stiff, and lightweight carbon-nanotube fibers. *Adv. Mater.* **2007,** *19* (23), 4198-4201.

(8) Janas, D.; Vilatela, A. C.; Koziol, K. K. K., Performance of carbon nanotube wires in extreme conditions. *Carbon* **2013,** *62*, 438-446.

(9) Kis, A.; Csanyi, G.; Salvetat, J.-P.; Lee, T.-N.; Couteau, E.; Kulik, A.; Benoit, W.; Brugger, J.; Forro, L., Reinforcement of single-walled carbon nanotube bundles by intertube bridging. *Nat. Mater.* **2004,** *3* (3), 153-157.

(10) Zhbanov, A. I.; Pogorelov, E. G.; Chang, Y.-C., Van der Waals interaction between two crossed carbon nanotubes. *Acs Nano* **2010,** *4* (10), 5937-5945.

(11) Buldum, A.; Lu, J. P., Contact resistance between carbon nanotubes. *PhyRvB* **2001,** *63* (16), 161403.

(12) Zhong, H.; Lukes, J. R., Interfacial thermal resistance between carbon nanotubes: molecular dynamics simulations and analytical thermal modeling. *Phys.Rev. B* **2006,** *74* (12), 125403.

(13) Li, Y. L.; Kinloch, I. A.; Windle, A. H., Direct spinning of carbon nanotube fibers from chemical vapor deposition synthesis. *Science* **2004,** *304* (5668), 276-278.

(14) Zou, J.; Zhang, X.; Zhao, J.; Lei, C.; Zhao, Y.; Zhu, Y.; Li, Q., Strengthening and toughening effects by strapping carbon nanotube cross-links with polymer molecules. *Compos. Sci. Technol.* **2016,** *135*, 123-127.

(15) Ma, W.; Song, L.; Yang, R.; Zhang, T.; Zhao, Y.; Sun, L.; Ren, Y.; Liu, D.; Liu, L.; Shen, J., Directly synthesized strong, highly conducting, transparent single-walled carbon nanotube films. *Nano Lett.* **2007,** *7* (8), 2307-2311.

(16) Wang, H.; Lu, W.; Di, J.; Li, D.; Zhang, X.; Li, M.; Zhang, Z.; Zheng, L.; Li, Q., Ultra-Lightweight and Highly Adaptive All-Carbon Elastic Conductors with Stable Electrical Resistance. *Adv. Funct. Mater.* **2017,** *27* (13), 1606220.

(17) Lekawa-Raus, A.; Kurzepa, L.; Peng, X.; Koziol, K., Towards the development of carbon nanotube based wires. *Carbon* **2014,** *68*, 597-609.

(18) Li, Q. W.; Li, Y.; Zhang, X. F.; Chikkannanavar, S. B.; Zhao, Y. H.; Dangelewicz, A. M.; Zheng, L. X.; Doorn, S. K.; Jia, Q. X.; Peterson, D. E.; Arendt, P. N.; Zhu, Y. T., Structure-Dependent Electrical Properties of Carbon Nanotube Fibers. *Adv. Mater.* **2007,** *19* (20), 3358-3363.

(19) Xu, G.; Zhao, J.; Li, S.; Zhang, X.; Yong, Z.; Li, Q., Continuous electrodeposition for lightweight, highly conducting and strong carbon nanotube-copper composite fibers. *Nanoscale* **2011,** *3* (10), 4215-4219.

(20) Alvarenga, J.; Jarosz, P. R.; Schauerman, C. M.; Moses, B. T.; Landi, B. J.; Cress, C. D.; Raffaelle, R. P., High conductivity carbon nanotube wires from radial densification and ionic doping. *Appl. Phys. Lett.* **2010,** *97* (18), 182106.

(21) Jarosz, P. R.; Shaukat, A.; Schauerman, C. M.; Cress, C. D.; Kladitis, P. E.; Ridgley, R. D.; Landi, B. J., High-Performance, Lightweight Coaxial Cable from Carbon Nanotube Conductors. *ACS Appl. Mater. Inter.* **2012,** *4* (2), 1103-1109.

(22) Zhao, J.; Li, Q.; Gao, B.; Wang, X.; Zou, J.; Cong, S.; Zhang, X.; Pan, Z.; Li, Q., Vibration-assisted infiltration of nano-compounds to strengthen and functionalize carbon nanotube fibers. *Carbon* **2016,** *101*, 114-119.

(23) Iijima, T.; Inagaki, Y.; Oshima, H.; Iwata, T.; Sato, R.; Kalita, G.; Kuzumaki, T.; Hayashi, Y.; Tanemura, M., Structural and Electrical Properties of Ozone Irradiated Carbon Nanotube Yarns and Sheets. *Mater. Express* **2012,** *2* (4), 357-362.

(24) Wang, X.; Behabtu, N.; Young, C. C.; Tsentalovich, D. E.; Pasquali, M.; Kono, J., High-Ampacity Power Cables of Tightly-Packed and Aligned Carbon Nanotubes. *Adv. Funct. Mater.* **2014,** *24* (21), 3241-3249.

(25) Li, Q. W.; Zhang, X. F.; DePaula, R. F.; Zheng, L. X.; Zhao, Y. H.; Stan, L.; Holesinger, T. G.; Arendt, P. N.; Peterson, D. E.; Zhu, Y. T., Sustained growth of ultralong carbon nanotube arrays for fiber spinning. *Adv. Mater.* **2006,** *18* (23), 3160-3163.

(26) Shang, Y.; Wang, Y.; Li, S.; Hua, C.; Zou, M.; Cao, A., High-strength carbon nanotube fibers by twist-induced self-strengthening. *Carbon* **2017,** *119*, 47-55.

(27) Subramaniam, C.; Yamada, T.; Kobashi, K.; Sekiguchi, A.; Futaba, D. N.; Yumura, M.; Hata, K., One hundred fold increase in current carrying capacity in a carbon nanotube-copper composite. *Nat. Commun.* **2013,** *4*, 2202.

(28) Han, B.; Guo, E.; Xue, X.; Zhao, Z.; Luo, L.; Qu, H.; Niu, T.; Xu, Y.; Hou, H., Fabrication and densification of high performance carbon nanotube/copper composite fibers. *Carbon* **2017**, *123*, 593-604.

(29) Lim, S. C.; Jang, J. H.; Bae, D. J.; Han, G. H.; Lee, S.; Yeo, I.-S.; Lee, Y. H., Contact resistance between metal and carbon nanotube interconnects: Effect of work function and wettability. *Appl. Phys. Lett.* **2009,** *95* (26), 264103.

(30) Shibuta, Y.; Maruyama, S., Bond-order potential for transition metal carbide cluster for the growth simulation of a single-walled carbon nanotube. *Comp. Mater. Sci.* **2007,** *39* (4), 842-848.

(31) Yukawa, S.; Sinnott, M. J., Grain Boundary Diffusion of Nickel into Copper. *JOM* **1955,** *7* (9), 996-1002.

(32) Lei, C.; Zhao, J.; Zou, J.; Jiang, C.; Li, M.; Zhang, X.; Zhang, Z.; Li, Q., Assembly dependent interfacial property of carbon nanotube fibers with epoxy and its enhancement via generalized surface sizing. *Adv. Eng. Mater.* **2016,** *18* (5), 839-845.

(33) Lu, L.; Shen, Y.; Chen, X.; Qian, L.; Lu, K., Ultrahigh Strength and High Electrical Conductivity in Copper. *Science* **2004,** *304* (5669), 422-426.

(34) Mehta, R.; Chugh, S.; Chen, Z., Enhanced electrical and thermal conduction in graphene-encapsulated copper nanowires. *Nano Lett.* **2015,** *15* (3), 2024-2030.

(35) Jiang, K.; Li, Q.; Fan, S., Nanotechnology: Spinning continuous carbon nanotube yarns. *Nature* **2002,** *419* (6909), 801-801.

(36) Liu, K.; Sun, Y.; Zhou, R.; Zhu, H.; Wang, J.; Liu, L.; Fan, S.; Jiang, K., Carbon nanotube yarns with high tensile strength made by a twisting and shrinking method. *Nanotechnology* **2009,** *21* (4), 045708.

(37) Li, S.; Zhang, X.; Zhao, J.; Meng, F.; Xu, G.; Yong, Z.; Jia, J.; Zhang, Z.; Li, Q., Enhancement of carbon nanotube fibres using different solvents and polymers. *Compos. Sci. Technol.* **2012,** *72* (12), 1402-1407.

TOC Graphic

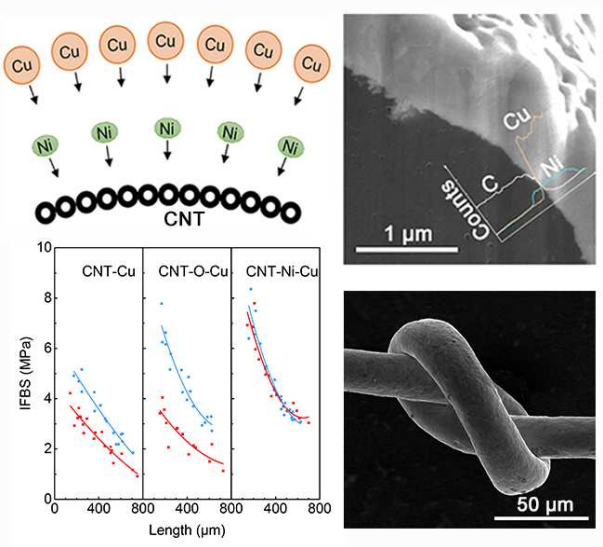


BRIEFS.

Coating CNT fiber with Cu layer is a feasible way to produce lightweight wire. However, weak CNT-Cu interaction significantly limited its mechanical and electrical properties. Here, we introduced a thin Ni buffer layer to solve this problem, producing a high-performance CNT-Ni-Cu fiber.